Incorporation of Iron Oxide Nanoparticles and Quantum Dots into Silica Microspheres

Numpon Insin,[†] Joseph B. Tracy,[†] Hakho Lee,[‡] John P. Zimmer,[†] Robert M. Westervelt,[‡] and Moungi G. Bawendi[†,*]

[†]Department of Chemistry, Massachusetts Institute of Technology, Cambridge, Massachusetts 02139, and [‡]Division of Engineering and Applied Sciences and Department of Physics, Harvard University, Cambridge, Massachusetts 02138

ABSTRACT We describe the synthesis of magnetic and fluorescent silica microspheres fabricated by incorporating maghemite (γ-Fe_2O_3) nanoparticles (MPs) and CdSe/CdZnS core/shell quantum dots (QDs) into a silica shell around preformed silica microspheres. The resultant ~500 nm microspheres have a narrow size distribution and show uniform incorporation of QDs and MPs into the shell. We have demonstrated manipulation of these microspheres using an external magnetic field with real-time fluorescence microscopy imaging.

KEYWORDS: silica microspheres · superparamagnetic · fluorescent · iron oxide nanoparticles · quantum dots · magnetic manipulation · multifunctional microspheres

Magnetic silica microspheres are of great interest for biomedical[1] and environmental research applications. Various kinds of magnetic microspheres have been used for bioseparation, drug targeting, cell isolation, enzyme immobilization, protein purification, and wastewater treatment.[2–4] Silica microspheres are of particular interest because of their biocompatibity and stability against degradation.[2,5,6] In addition, silica microspheres can be easily modified with a wide range of functional groups.[6] Consequently, magnetic silica microspheres have been widely studied by many techniques, such as layer-by-layer self-assembly,[2] the Stöber process,[7] ferrite plating,[8] aerosol pyrolysis,[9] and sonochemical deposition.[10]

For the preparation of magnetic silica microspheres, incorporation of ferromagnetic or ferrimagnetic nanoparticles is desirable. These magnetic nanoparticles (MPs) range in size from a few nanometers to tens of nanometers. Sufficiently small MPs in this size regime exist as single-domain magnets,[11] in which each MP has a constant magnetic moment that can be reoriented in an applied field. When small MPs are heated from low temperature, thermal energy begins to perturb their moments' orientational stability, which is known as superparamagnetism. Superparamagnetic MP moments can be oriented in an applied field, but they have no net magnetization in zero field. The onset of superparamagnetism is gradual, and the blocking temperature (T_B), which is proportional to the MP volume, demarcates the transition to superparamagnetism. Small, superparamagnetic MPs with low T_B are much less susceptible to aggregation than larger ones. MPs have been utilized in various biomedical applications, such as magnetic separation, drug delivery, magnetic resonance imaging (MRI), and hyperthermia cancer treatment.[1,12] Among MPs, maghemite (γ-Fe_2O_3) is promising for *in vivo* applications because of the known biocompatibility of γ-Fe_2O_3.[12]

Incorporating MPs along with chromophores enables additional applications. Such microspheres can be moved with an external magnetic field while monitoring their motion through fluorescence in real time.[13,14] Fluorescent and magnetic microspheres have previously been fabricated by combining magnetic nanoparticles with organic dyes or lanthanide metal complexes.[13,14] Advantages of using QDs as fluorophores are their continuous adsorption spectra, narrow emission bandwidths, and large two-photon absorption cross-section.[15–17]

Simultaneously magnetic and luminescent composite silica microspheres containing both MPs and QDs have attracted great interest.[5,6,18,19] Previous fabrication methods included the use of MPs and QDs as cores followed by the growth of a silica shell,[6,18] and the inverse suspension method.[5] However, most samples prepared using these methods were polydisperse.[5,18] Moreover, the numbers of

See the accompanying perspective by Halas on p 179.

*Address correspondence to mgb@mit.edu.

Received for review November 2, 2007 and accepted December 05, 2007.

Published online January 10, 2008.
10.1021/nn700344x CCC: $40.75

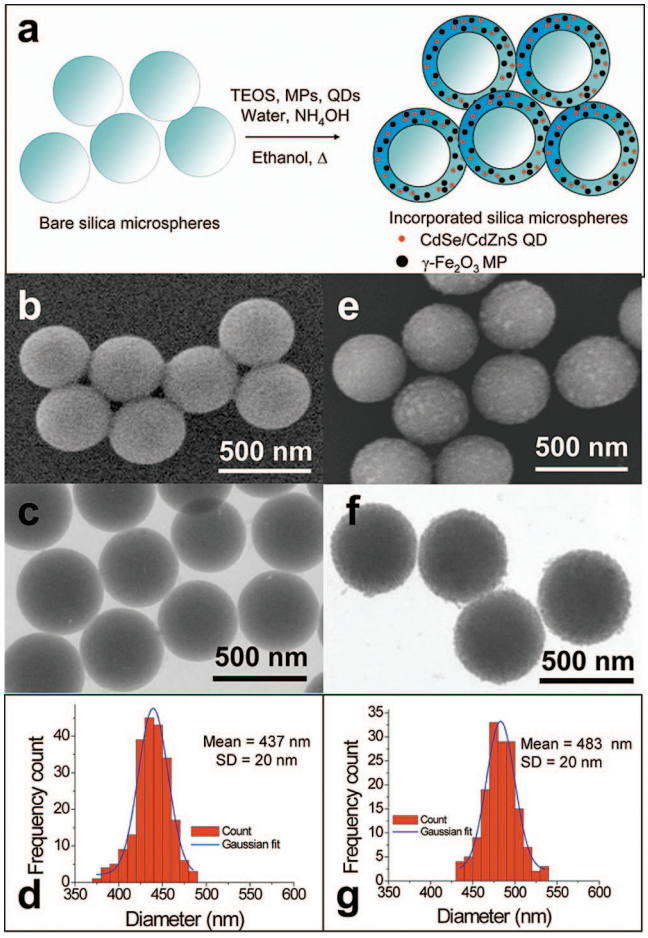

Figure 1. (a) Reaction scheme for the functionalization of silica microspheres; (b) SEM image, (c) TEM image, and (d) size distribution analysis of 500 nm silica microspheres (Polysciences, 500 ± 70 nm) before incorporation of QDs and MPs; and (e) SEM image, (f) TEM image, and (g) size distribution analysis of 500 nm silica microspheres after incorporation of QDs and MPs (7 nm MP, 12 000 MPs per microsphere).

MPs and QDs in each composite particle within the same sample were not uniform.[5,6,18] More recently, magnetic and fluorescent silica microspheres were prepared by using silica-coated MPs as cores, followed by layer-by-layer (LbL) assembly of polyelectrolytes and QDs onto the cores' surfaces, which were then coated with a final silica shell.[19] However, the size dispersity of the particles was not characterized, and the MP content in each microsphere was limited and uncontrolled. In addition, the technique of polyelectrolyte-assisted QD assembly limited the number of QDs adsorbed onto the cores' surfaces to a monolayer. This technique also used QDs with negatively charged surfaces prepared with an aqueous method,[20] which was known to yield QDs with poorer crystallinity, monodispersity, and fluorescence efficiency than QDs prepared in nonaqueous coordinating solvents using the "hot-injection" technique.[20,21]

Here we report the synthesis of monodisperse silica microspheres with MPs and QDs both uniformly incorporated and demonstrate their practical bifunctionality. Potential applications of these microspheres include monitoring drug delivery and the combination of deep-tissue MRI with high-resolution confocal laser scanning microscopy.

Our approach is based on our previous work, in which QDs were incorporated into silica shells grown on prefabricated silica microsphere cores through a sol–gel process.[15] This fabrication method maintains the monodisperse microsphere size and QD optical properties, and the nanoparticles are incorporated uniformly into the microspheres' shells. We have modified the microspheres' shells to include not only QDs but MPs as well. Preparation of the nanoparticle stock solution is the critical fabrication step. Both the QDs and MPs must be highly soluble in ethanol and also possess accessible alkoxysilane groups, which polymerize with tetraethoxysilane (TEOS) to form the shell.

Scanning electron microscopy (SEM) and transmission electron microscopy (TEM) show that the morphology of the core microspheres (Figure 1b,c) did not change during growth of the of QD- and MP-doped shells (Figure 1e,f), but rougher surfaces were observed. The increase in surface roughness may result in changes in biocompatibility and toxicity of the resulting microspheres compared with bare ones. This will need to be studied before utilizing these microspheres in biological applications. Size distributions (Figure 1d,g) measured from TEM indicate that the incorporation process did not significantly affect the size dispersity of the microspheres. Moreover, the increase in average size of the overcoated microspheres confirmed that the core/shell structure was formed.

As noted above, the crucial step for incorporating MPs into silica microspheres was the preparation of the MP stock solution in ethanol. The MPs' native surfactant, oleic acid, was displaced by 5-amino-1-pentanol (AP) and 3-aminopropyltrimethoxysilane (APS) in order for the MPs to become ethanol-soluble and polymerizable with TEOS. Addition of a small amount of 12-hydroxydodecanoic acid (HDDA) helped to facilitate MP solubility and incorporation into the microspheres. For instance, in the incorporation of 7 nm MPs into 500 nm microspheres, the MP content was as high as 13 000 MPs per microsphere when HDDA was added to the MP solution. Without HDDA, however, the highest MP content achievable before the aggregation of MPs outside the microspheres was four times less. We attribute the improved incorporation to the increased solubility of MPs in ethanol, which could reduce the rate of self-condensation of APS, and was probably the reason for MP aggregation outside microspheres.

Other ligand systems that are similar in structure to HDDA were also explored. Some shorter carbon chain hydroxycarboxylic acids, such as DL-α-hydroxycaproic acid and 6-hydroxycaproic acid, were less effective in dispersing MPs into ethanol and yielded a lower MP loading into the microspheres. Ligands with different

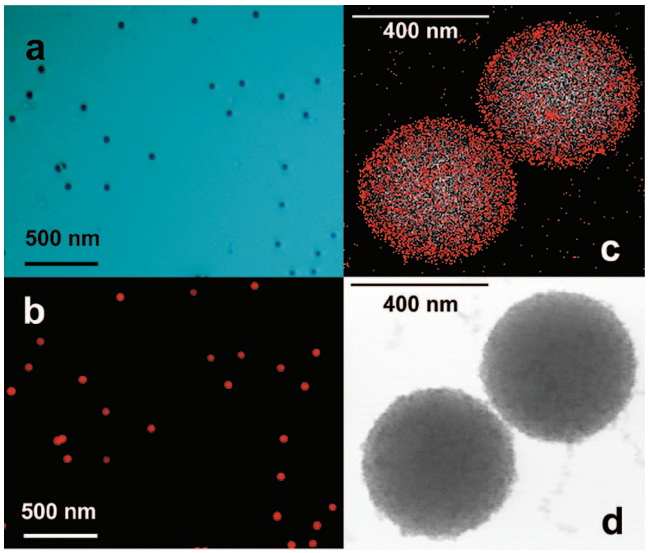

Figure 2. Images of the microspheres from an optical microscope, (a) transmission image and (b) fluorescence image of the same area, and from STEM, (c) distribution map of silicon (white spots) and iron (red spots) and (d) transmission image of microspheres shown in panel c.

functional groups such as 12-amino-1-dodecanol were also investigated, but HDDA gave the best results in terms of MP dispersibility and loading.

Fluorescence microscopy showed that the microspheres were suitably bright for imaging applications. In particular, every microsphere exhibited QD fluorescence of similar intensities, implying that the QDs were incorporated and distributed uniformly as seen in Figure 2a,b.

The distribution of iron was observed using scanning transmission electron microscopy (STEM) equipped with an energy-dispersive X-ray analyzer, as shown in Figure 2c. Uniform distribution among many microspheres was observed. Moreover, this plot of iron (red spots) and silicon atoms (white spots), identified the shell as the area of dense distribution of iron atoms. This observation, combined with data from a line scanning across a single microsphere (see Supporting Information), indicated a shell thickness of 55 ± 10 nm.

The numbers of QDs and MPs incorporated in each microsphere were determined by elemental analysis using inductively coupled plasma optical emission spectroscopy (ICP-OES) performed by Galbraith Laboratories, Inc. For 500 nm microspheres, QDs accounted for 1.1% ± 0.3% of the total volume or 2.0% ± 1.2% of the shell volume, which corresponds to 4600 ± 1400 QDs per microsphere. The highest percent volume of MPs was 3.9% ± 1.1% of the total volume or 7.3% ± 4.1% of the shell. This amount corresponds to 13 000 ± 3700 MPs per 500 nm microsphere (see Supporting Information for details).

The magnetic properties of these microspheres were measured using a SQUID magnetometer. Figure 3a shows the magnetization versus magnetic field at 5 K for three different microsphere samples. From the shapes of the hysteresis loops, it can be inferred that microspheres containing both MPs and QDs were ferromagnetic at 5 K (green and black lines in Figure 3a), while the microspheres with only QDs incorporated were diamagnetic (pink line). Moreover, the value of the saturation magnetization (M_S) of each sample was measured and used to estimate the amount of γ-Fe_2O_3 in each sample based on the known M_S of bulk γ-Fe_2O_3 (3.9×10^5 A m^{-1}).[22] The number of incorporated MPs per microsphere was estimated using the diameter of the microspheres and MPs measured from TEM images, the mass of the sample, and the assumption that MPs were uniformly incorporated and did not significantly alter the density of bulk SiO_2. Accordingly, 500 nm microspheres with 7 nm MPs incorporated exhibited a M_S of 5.35 emu/g and thus contained 11 000 ± 3100 MPs per microsphere. This number of MPs is 20% lower than that obtained from ICP-OES elemental analysis. The higher number is probably more reliable, because size[23] and ligand effects[24] cause M_S of MPs to be lower than that of bulk maghemite.

In Figure 3b, T_B corresponds to the maximum in the zero-field cooled magnetization curves measured in a small field (100 Oe). As the MP concentration in-

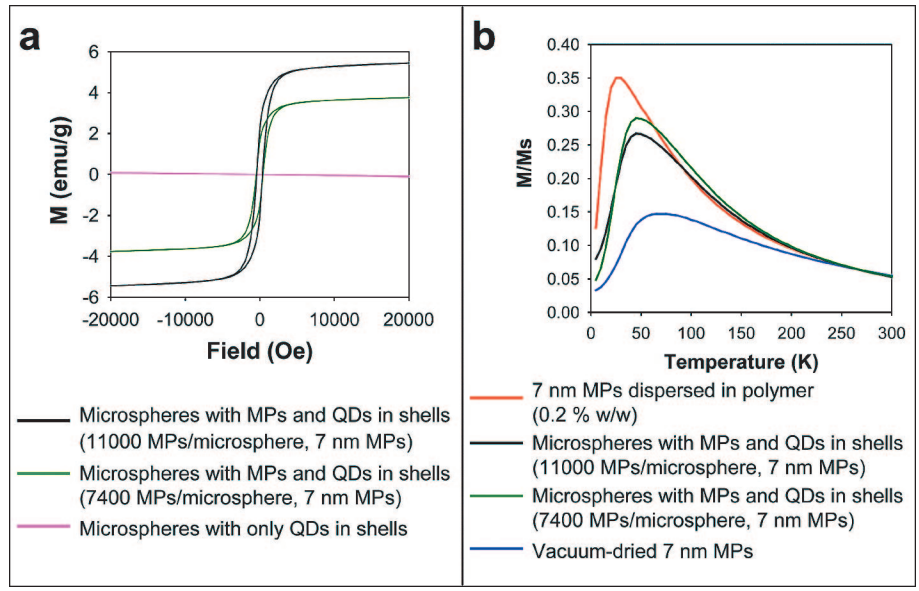

Figure 3. Magnetic characterization of the 500 nm microspheres: (a) magnetization versus magnetic field at 5 K; (b) zero-field cooled magnetization versus temperature measured in a 100 Oe field.

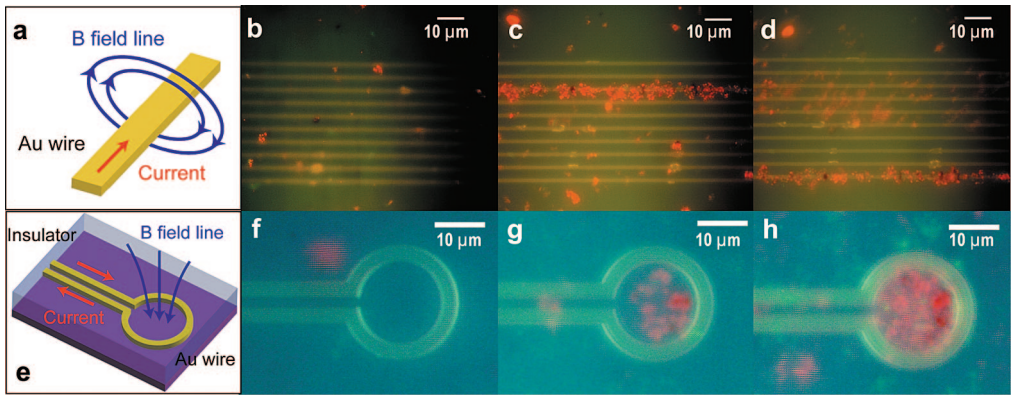

Figure 4. Images of trapping on two microelectromagnetic devices, (a–d) an array of parallel wires and (e–f) ring trap: (a) the current flow and magnetic field from the wires; (b) no current in wires; (c) third wire from the top turned on; (d) bottom wire turned on; (e) the current flow and magnetic field from the ring; (f) no current; (g) after the ring current was turned on for 1 min; (h) after the ring current was turned on for 6 min.

creases, the dipolar interaction between MPs becomes stronger, which causes T_B to increase and the magnetization at low temperature to decrease. At high temperature, the normalized temperature-dependent magnetization curves for samples of different concentrations converge when thermal energy has overcome interparticle dipolar coupling. As a reference in which dipolar coupling was negligible,[25] we prepared a sample of MPs dispersed in poly(laurylmethacrylate) cross-linked with ethylene glycol dimethacrylate.[26] As shown in Figure 3b, MPs dispersed in polymer have a blocking temperature of 30 K (red line), while the magnetic microspheres have T_B of 45–50 K (green and black lines). The increase in T_B indicates that the packing density of the MPs in the microspheres was higher than that of the MPs dispersed in polymer.[25] However, when compared with vacuum-dried MPs, whose T_B is 70 K (blue line), the MPs in the microspheres had a lower T_B, which indicates that the packing density of the MPs in microspheres was still not as high as that of the dried powder MPs.

As a demonstration of the combined magnetic and fluorescence characteristics of the microspheres, we have performed the magnetic manipulation of the microspheres in a liquid. Microelectromagnets, which are lithographically patterned conducting wires, were used to control the motion of microspheres.[27] Local magnetic fields generated by microelectromagnets interact with MPs in the microspheres and pull them toward the maximum in the field magnitude. Two types of microelectromagnets, an array of wires and a ring trap, were fabricated for this demonstration. The manipulation process can be easily monitored in real time by observing the emission from QDs in the microspheres.

When an external magnetic field **B** is generated by microelectromagnets, the microspheres assume induced magnetic moments $\mathbf{m} = \chi V\mathbf{B}/\mu_o$, where χ and V are the magnetic susceptibility and the volume of the microspheres, respectively, and μ_o is the permeability of vacuum. Subsequent interactions between **B** and **m** pull the microspheres toward the maximum in the magnetic field magnitude where the microspheres are trapped. The trapping potential energy of microspheres is $U = -(1/2)\mathbf{m}\cdot\mathbf{B} = -(1/2)\chi VB^2/\mu_o$, and microspheres remain trapped provided $|U| > k_BT$, where k_B is the Boltzmann constant and T is the temperature. This condition sets the criterion on the minimum magnetic field magnitude $B_m = (2\mu_o k_BT/(\chi V))^{1/2}$ required for trapping at a given temperature. The microspheres used in this experiment have $\chi = 0.53$ (see Supporting Information) and $V = 5.9 \times 10^7$ nm^3, which gives $B_m = 6$ G at $T = 300$ K. These microelectromagnetic devices can readily generate magnetic fields >30 G, which ensures stable trapping of microspheres in liquids.

For straight wires, the maximum magnetic field is located around the current-carrying wire (Figure 4a). Before the current was turned on, the red-emitting microspheres floated randomly over an array of wires (Figure 4b). After the third wire from the top was activated, the microspheres were immediately attracted to the third wire (Figure 4c). After the third wire was turned off, the bottom wire was switched on (Figure 4d). Additional microspheres were attracted to the bottom wire, and the cloud of microspheres shown between the third and sixth (from the top) wires, which had been trapped on the third wire, were later trapped on the bottom wire. This experiment shows that the microspheres respond to small magnetic field gradients, because the microspheres that were on the third bar moved to the bottom bar from more than 50 μm away.

In experiments using a ring trap, we used two different types of microspheres, green-emitting microspheres without MPs incorporated and red-emitting microspheres with MPs incorporated. (The green-emitting microspheres were in relatively low concentration, and they are difficult to discern against the background in this experiment.) In this device, the magnetic field maximum was in the middle of the ring, as shown in Figure 4e. When there was no current, both green and red microspheres floated freely over the device (Figure 4f). One minute after turning on the ring current, red-emitting microspheres were attracted to the middle of the ring (Figure 4g); more were attracted after longer on-times (Figure 4h). The green-emitting microspheres, in contrast, still floated randomly.

In conclusion, we have developed a new type of luminescent silica microsphere with a tight size distribution that responds to magnetic fields by incorporating MPs and QDs into the silica shells of the prefabricated microspheres. We have also demonstrated the bifunctionality of the microspheres by manipulating them using external magnetic fields with real-time fluorescence monitoring. These microspheres have potential for biomedical applications as a probe that responds to magnetic field gradients and simultaneously luminesces.

METHODS

Characterization. Fluorescence images of the microspheres were obtained using a Nikon Eclipse ME600 epifluorescence optical microscope equipped with a Nikon DXM1200 digital camera. In order to obtain uniformly distributed microspheres for light microscope imaging, we prepared samples by spin coating the microspheres dispersed in ethanol onto glass microscope slides. TEM images of the microspheres were obtained with a JEOL 200CX electron microscope operated at 200 kV. SEM images were obtained using a FEI/Philips XL30 field-emission gun environmental scanning electron microscope (FEG-ESEM) at an acceleration voltage of 20 kV. Elemental mapping and line scanning were done using a VG HB603 scanning transmission electron microscope operating at 250 kV equipped with a Link Systems energy-dispersive X-ray analyzer. Magnetometry was performed with a SQUID (Quantum Design MPMS-5S).

Preparation of MP and QD Stock Solutions in Ethanol. CdSe/ZnS and CdSe/CdZnS core/shell QDs were prepared in a two-step synthesis, similar to our previous work.[28] Maghemite (γ-Fe_2O_3) magnetic nanoparticles (MPs) were prepared using a method modified from the literature.[29,30] As an example, for the synthesis of 7 nm MPs, 400 μL of $Fe(CO)_5$ was added to 2 mL of oleic acid in 20 mL of dioctyl ether at 100 °C. The temperature was increased at a rate of 2 °C/min to a final temperature of 275 °C, at which it was held constant for 1.5 h. After the mixture was cooled to room temperature, 0.30 g of $(CH_3)_3NO$ was added as an oxidizing agent. The mixture was heated to 130 °C for 2 h and was then heated to 275 °C for 15 min. After cooling, the MPs were processed for storage by first adding ethanol to precipitate them. After centrifuging, the supernatant was discarded, and the MPs were then redispersed and kept in hexanes. The MP particle size was controlled by varying the molar ratio of $Fe(CO)_5$ to oleic acid and the duration of heating at 275 °C prior to addition of $(CH_3)_3NO$.

The QD stock solution in ethanol was prepared using a previously reported technique.[15] In a typical procedure, as-synthesized QDs were precipitated twice with a methanol/butanol mixture to remove their native trioctylphosphine oxide (TOPO) caps and were dried under vacuum. Next, 26 mg of dried QDs was mixed with 195 mg of anhydrous ethanol, 29 mg of 3-aminopropyltrimethoxysilane (APS), and 54 mg of 5-amino-1-pentanol (AP). The mixture was then heated to 40 °C for about 1 h, leading to the formation of a solution of QDs.

The MP stock solution in ethanol was prepared by two slightly different procedures. The first procedure was the same as the preparation of QD solution mentioned above, with three times more AP added. In the second procedure, more delicate but yielding higher MP content, the MP stock solution in ethanol was prepared using addition of 12-hydroxydodecanoic acid, sonication, and syringe filtration. For example, the MPs kept in hexanes were precipitated using ethanol to remove their native oleic acid caps and were then dried under vacuum. Then, 47 mg of dried MPs, 95 mg of 12-hydroxydodecanoic acid, and 1.49 g of ethanol were sonicated for 1 h, yielding a clear solution of MPs. AP (418 mg) and APS (772 mg) were then added to the MP solution, and the mixture was heated to 40 °C for 1 h to ensure cap exchange with AP and APS. The mixture was then filtered through a 20-μm syringe filter, leading to a solution of MPs.

Incorporation of QDs and MPs into Silica Microspheres. The procedure for incorporating MPs and QDs together into silica microspheres was adapted from Chan *et al.*[15] In a typical procedure, 30 mg of bare silica microspheres and 16 mg of hydroxypropyl cellulose (HPC) were added to 10 mL of ethanol, and this mixture was sonicated for 10 min. MP solution (50–500 μL) and 10 μL of QD solution were added to the reaction mixture while the solution was vigorously stirred, followed by the addition of 50 μL of H_2O, 50 μL of NH_4OH, (28 wt% in H_2O) and 0.15 mL of TEOS. The mixture was stirred in an oil bath at 75 °C for 4 h. The silica (core)/silica−MPs−QDs (shell) microspheres were then purified by performing five cycles of centrifuging, discarding the supernatant, and redispersing the microspheres in ethanol. The reaction scheme for this process is shown in Figure 1a.

Demonstration of Trapping of the Microspheres with External Magnetic Fields. The fabrication process for the microelectromagnets was previously reported.[31] Two types of devices used in this work were arrays of Au wires (Figure 4a) and a Au wire patterned into a ring (Figure 4e). The maximum current used in these experiments was 0.09 A, corresponding to magnetic field of ~67 G on the surface of the wires in the parallel wire array and ~42 G in the middle of the ring trap. In these trapping experiments, we used microspheres dispersed in water instead of ethanol to avoid rapid evaporation of the solvent. The microspheres were transferred from the ethanol medium to a water medium by two cycles of centrifugation and redispersion into water.

Acknowledgment. We thank A. J. Garratt-Reed for the scanning transmission electron microscopy work, A. Dorn for scanning electron microscopy assistance, Y. Chan, D. C. Oertel, G. P. Nair, and P. T. Snee for helpful discussions, and the Anandamahidol Foundation (Thailand) for a graduate fellowship awarded to N.I. This work was funded in part through the National Science Foundation Materials Research Science and Engineering Center (NSF MRSEC) program at MIT, the MIT-Harvard NIH Center for Cancer Nanotechnology Excellence (1U54-CA119349), the NSF Nanoscale Science and Engineering Center (NSF NSEC program) at Harvard University, and a grant from the Human Frontier Science Program (RGP0005/2007-C).

Supporting Information Available: Determination of microspheres shell thickness, calculation of MP and QD content in microspheres from ICP-OES elemental analysis and saturation magnetization measurement, and calculation of magnetic susceptibility of a microsphere used in trapping experiment. This material is available free of charge *via* the Internet at http://pubs.acs.org.

REFERENCES AND NOTES

1. Pankhurst, Q. A.; Connolly, J.; Jones, S. K.; Dobson, J. Applications of Magnetic Nanoparticles in Biomedicine. *J. Phys. D: Appl. Phys.* **2003**, *36*, R167–R181.
2. Zhu, Y. H.; Da, H.; Yang, X. L.; Hu, Y. Preparation and Characterization of Core-Shell Monodispersed Magnetic Silica Microspheres. *Colloids Surf., A* **2003**, *231*, 123–129.
3. Yang, C. L.; Guan, Y. P.; Xing, J. M.; Liu, J. G.; Shan, G. B.; An, Z. T.; Liu, H. Z. Preparation of Magnetic Polystyrene Microspheres with a Narrow Size Distribution. *AIChE J.* **2005**, *51*, 2011–2015.
4. Tanyolac, D.; Ozdural, A. R. Preparation of Low-Cost Magnetic Nitrocellulose Microbeads. *React. Funct. Polym.* **2000**, *45*, 235–242.
5. Muller-Schulte, D.; Schmitz-Rode, T.; Borm, P. Ultra-Fast Synthesis of Magnetic and Luminescent Silica Beads for Versatile Bioanalytical Applications. *J. Magn. Magn. Mater.* **2005**, *293*, 135–143.
6. Yi, D. K.; Selvan, S. T.; Lee, S. S.; Papaefthymiou, G. C.; Kundaliya, D.; Ying, J. Y. Silica-Coated Nanocomposites of Magnetic Nanoparticles and Quantum Dots. *J. Am. Chem. Soc.* **2005**, *127*, 4990–4991.

7. Claesson, E. M.; Philipse, A. P. Monodisperse Magnetizable Composite Silica Spheres with Tunable Dipolar Interactions. *Langmuir* **2005**, *21*, 9412–9419.
8. Zhang, M. J.; Itoh, T.; Abe, M. Ultrasonic Visualization of Still and Flowing Waters Using Contrast Agents of Magnetite-Encapsulated Porous Silica Microspheres. *Jpn. J. Appl. Phys., Part 1* **1997**, *36*, 243–246.
9. Tartaj, P.; Gonzalez-Carreno, T.; Bomati-Miguel, O.; Serna, C. J.; Bonville, P. Magnetic Behavior of Superparamagnetic Fe Nanocrystals Confined inside Submicron-Sized Spherical Silica Particles. *Phys. Rev. B* **2004**, *69*, 094401.
10. Ramesh, S.; Prozorov, R.; Gedanken, A. Ultrasound Driven Deposition and Reactivity of Nanophasic Amorphous Iron Clusters with Surface Silanols of Submicrospherical Silica. *Chem. Mater.* **1997**, *9*, 2996–3004.
11. Krishnan, K. M.; Pakhomov, A. B.; Bao, Y.; Blomqvist, P.; Chun, Y.; Gonzales, M.; Griffin, K.; Ji, X.; Roberts, B. K. Nanomagnetism and Spin Electronics: Materials, Microstructure and Novel Properties. *J. Mater. Sci.* **2006**, *41*, 793–815.
12. Gupta, A. K.; Gupta, M. Synthesis and Surface Engineering of Iron Oxide Nanoparticles for Biomedical Applications. *Biomaterials* **2005**, *26* (18), 3995–4021.
13. Yoon, T. J.; Kim, J. S.; Kim, B. G.; Yu, K. N.; Cho, M. H.; Lee, J. K. Multifunctional Nanoparticles Possessing a "Magnetic Motor Effect" for Drug or Gene Delivery. *Angew. Chem., Int. Ed.* **2005**, *44*, 1068–1071.
14. Qiu, G. M.; Xu, Y. Y.; Zhu, B. K.; Oiu, G. L. Novel, Fluorescent, Magnetic, Polysaccharide-Based Microsphere for Orientation, Tracing, and Anticoagulation: Preparation and Characterization. *Biomacromolecules* **2005**, *6*, 1041–1047.
15. Chan, Y.; Zimmer, J. P.; Stroh, M.; Steckel, J. S.; Jain, R. K.; Bawendi, M. G. Incorporation of Luminescent Nanocrystals into Monodisperse Core-Shell Silica Microspheres. *Adv. Mater.* **2004**, *16*, 2092–2097.
16. Hong, X.; Li, J.; Wang, M. J.; Xu, J. J.; Guo, W.; Li, J. H.; Bai, Y. B.; Li, T. J. Fabrication of Magnetic Luminescent Nanocomposites by a Layer-by-Layer Self-Assembly Approach. *Chem. Mater.* **2004**, *16*, 4022–4027.
17. Fu, A. H.; Gu, W. W.; Larabell, C.; Alivisatos, A. P. Semiconductor Nanocrystals for Biological Imaging. *Curr. Opin. Neurobiol.* **2005**, *15*, 568–575.
18. Kim, J.; Lee, J. E.; Lee, J.; Yu, J. H.; Kim, B. C.; An, K.; Hwang, Y.; Shin, C. H.; Park, J. G.; Hyeon, T. Magnetic Fluorescent Delivery Vehicle Using Uniform Mesoporous Silica Spheres Embedded with Monodisperse Magnetic and Semiconductor Nanocrystals. *J. Am. Chem. Soc.* **2006**, *128*, 688–689.
19. Salgueirino-Maceira, V.; Correa-Duarte, M. A.; Spasova, M.; Liz-Marzan, L. M.; Farle, M. Composite Silica Spheres with Magnetic and Luminescent Functionalities. *Adv. Funct. Mater.* **2006**, *16*, 509–514.
20. Gaponik, N.; Radtchenko, I. L.; Sukhorukov, G. B.; Rogach, A. L. Luminescent Polymer Microcapsules Addressable by a Magnetic Field. *Langmuir* **2004**, *20*, 1449–1452.
21. Smith, A. M.; Ruan, G.; Rhyner, M. N.; Nie, S. M. Engineering Luminescent Quantum Dots for in Vivo Molecular and Cellular Imaging. *Ann. Biomed. Eng.* **2006**, *34*, 3–14.
22. Tepper, T.; Ross, C. A. Pulsed Laser Deposition of Iron Oxide Films. *J. Appl. Phys.* **2002**, *91*, 4453–4456.
23. Berkowitz, A. E.; Schuele, W. J.; Flanders, P. J. Influence of Crystallite Size on the Magnetic Properties of Acicular Gamma-Fe_2O_3 Particles. *J. Appl. Phys.* **1968**, *39*, 1261–1263.
24. Berkowitz, A. E.; Lahut, J. A.; Jacobs, I. S.; Levinson, L. M.; Forester, D. W. Spin Pinning at Ferrite-Organic Interfaces. *Phys. Rev. Lett.* **1975**, *34*, 594–597.
25. Frankamp, B. L.; Boal, A. K.; Tuominen, M. T.; Rotello, V. M. Direct Control of the Magnetic Interaction Between Iron Oxide Nanoparticles through Dendrimer-Mediated Self-Assembly. *J. Am. Chem. Soc.* **2005**, *127*, 9731–9735.
26. Tracy, J. B.; Weiss, D. N.; Dinega, D. P.; Bawendi, M. G. Exchange Biasing and Magnetic Properties of Partially and Fully Oxidized Colloidal Cobalt Nanoparticles. *Phys. Rev. B* **2005**, *72*, 064404.
27. Lee, C. S.; Lee, H.; Westervelt, R. M. Microelectromagnets for the Control of Magnetic Nanoparticles. *Appl. Phys. Lett.* **2001**, *79*, 3308–3310.
28. Fisher, B. R.; Eisler, H. J.; Stott, N. E.; Bawendi, M. G. Emission Intensity Dependence and Single-Exponential Behavior in Single Colloidal Quantum Dot Fluorescence Lifetimes. *J. Phys. Chem. B* **2004**, *108*, 143–148.
29. Woo, K.; Hong, J.; Choi, S.; Lee, H. W.; Ahn, J. P.; Kim, C. S.; Lee, S. W. Easy Synthesis and Magnetic Properties of Iron Oxide Nanoparticles. *Chem. Mater.* **2004**, *16*, 2814–2818.
30. Teng, X. W.; Yang, H. Effects of Surfactants and Synthetic Conditions on The Sizes and Self-Assembly of Monodisperse Iron Oxide Nanoparticles. *J. Mater. Chem.* **2004**, *14*, 774–779.
31. Lee, H.; Purdon, A. M.; Westervelt, R. M. Micromanipulation of Biological Systems with Microelectromagnets. *IEEE Trans. Magn.* **2004**, *40*, 2991–2993.